Renormalization of *NN* scattering with one pion exchange and energy dependent boundary conditions

M. Pavón Valderrama* and E. Ruiz Arriola†
Departamento de Física Moderna, Universidad de Granada, E-18071 Granada, Spain
(Received 20 May 2004; revised manuscript received 11 July 2004; published 29 October 2004)

A nonperturbative renormalization scheme for nucleon-nucleon interaction based on boundary conditions at short distances is presented and applied to the one pion exchange potential. It is free of off-shell ambiguities and ultraviolet divergences, provides finite results at any step of the calculation, and allows us to remove the short distance cutoff in a suitable way. Low energy constants and their nonperturbative evolution can be directly obtained from experimental threshold parameters in a completely unique and model independent way when the long range explicit pion effects are eliminated. This allows us to compute scattering phase shifts which are, by construction, consistent with the effective range expansion to a given order in the center of mass (c.m.) momentum p. In the singlet $^1S_0$ and triplet $^3S_1$-$^3D_1$ channels ultraviolet fixed points and limit cycles are obtained, respectively, for the threshold parameters. Data are described satisfactorily up to c.m. momenta of about $p \sim m_\pi$.

DOI: 10.1103/PhysRevC.70.044006 PACS number(s): 03.65.Nk, 11.10.Gh, 13.75.Cs, 21.30.Fe

I. INTRODUCTION

Effective field theories (EFT) are a powerful tool to deal with nonperturbative low energy physics. Over the last years, they have provided promising results as regards a systematic and model independent understanding of hadronic and nuclear physics. The scale separation between long and short distance physics makes the development of a systematic power counting possible. After the original proposal of Weinberg [1] to design power counting based on applying chiral perturbation theory (ChPT) to the potential, many works have followed, implementing such a counting [2–4,48] with finite cutoffs or proposing a counting in the renormalized S matrix [5,6] which has also been pursued to NNLO [7]. The relation of both the Weinberg (W) and Kaplan-Savage-Wise (KSW) counting has been understood as perturbative expansions about infrared fixed points in the limit of small and large scattering lengths [8], respectively (see also Refs. [9,10] for a discussion on long range forces in that context). For systems with a large scattering length, as it turns out to be the case in low energy *NN* scattering, the Weinberg counting may be modified to iterate the scattering length to all orders, but then the connection to ChPT must be given up [12]. On the other hand the KSW counting, although systematic, does not converge at NNLO [7]. In Ref. [13] a new counting [Beane, Bedaque, Savage, and van Kolck (BBSvK)] involving also the chiral limit should be invoked. According to these authors, one should treat nonperturbatively the *NN* potential in the chiral limit and consider finite pion mass corrections perturbatively on top of that. For a recent and more complete review on these and related issues see, e.g., Ref. [14] and references therein. More recent works supporting the W counting have also appeared [15,16].

The practical problem one encounters within *NN* scattering is the disentanglement between short and long range physics in a nonperturbative and model independent way. As we will show in this paper such a separation can be achieved using renormalization group ideas. However, the issue of regularization and renormalization in the present context is not at all trivial, particularly if the calculation involves summing up some infinite set of diagrams (see, e.g., the discussions in Refs. [17–20]). From a diagrammatic point of view momentum space treatments based on nonperturbative analysis of the Lippmann-Schwinger equation [4,21–27] are more natural within a Lagrangian framework and allow explicit consideration of nonlocal potentials. On the other hand, the long range *NN* potentials making use of chiral symmetry constraints are local, and for those the analysis of nonperturbative renormalization in coordinate space becomes much simpler, as will be shown along this work. In addition, the Schrödinger equation is a second order operator and mixed boundary conditions define a complete and unique solution of the scattering problem in the whole space at both sides of the boundary. This sharp boundary separation of the space is naturally formulated in coordinate space for a local potential. Boundary conditions for *NN* scattering were used many years ago (see, e.g., Ref. [28] and references therein), and there has been renewed interest motivated by the developments within EFT [29–31]. Actually, the thorough analysis of Ref. [31] shows that in the absence of long range forces a low momentum expansion of the potential within EFT framework for the Lippmann-Schwinger equation is completely equivalent to an effective range expansion (ERE) [32] and also to an energy expansion of a generic boundary condition at the origin in coordinate space for the Schrödinger equation. Moreover, the reference partial wave analysis of the Nijmegen group [33,34] uses this method to successfully describe the large *NN* scattering database, when long range potentials are used. While in the first works phenomenological potentials were used, more recent studies consider potentials deduced from ChPT with a rather satisfactory description of the experimental scattering data [35]. The minimal boundary radius that can still provide an acceptable χ^2/degree of freedom is about $R_S = 1.4-1.8$ fm. Obviously, if

*Electronic address: mpavon@ugr.es
†Electronic address: earriola@ugr.es

the radius cannot be lowered without spoiling the quality of the fit, the short distance cutoff becomes an indispensable parameter of the theory, which cannot be removed. The corresponding momentum space cutoff $\Lambda = 2\pi/R_S \sim 600$ MeV is comparable to the one needed in early momentum space treatments [4]. Within the spirit of an EFT it would actually be more appropriate to take instead larger Λ's or equivalently shorter R_S's and to check for insensitivity of results in the low energy regime. Thus, there arises the natural question whether in fact the EFT program can be implemented regardless of any finite cutoff.

In our previous work [36] we showed that for the $^1S_0$ singlet channel with OPE the boundary radius can be effectively removed without spoiling a good description of the corresponding phase shift up to the *a priori* expected center of mass (c.m.) momentum of $k \sim m_\pi$ where the two pion exchange (TPE) effects should start playing a role. The first order differential equation satisfied by the boundary condition of the problem defined in the interval $R < r < \infty$ as a function of the boundary radius was very helpful, since the whole problem could be mapped into a variable phase equation [37] of a truncated potential in the region $0 < r \leqslant R$ with a nontrivial initial condition at the origin, encoding the short distance physics. In this way, the long range pions could be eliminated and the evolution of the threshold parameters as a function of the boundary radius could be determined nonperturbatively. Actually, a trivial ultraviolet fixed point limit for the scattering length was found nonperturbatively. Remarkably, this behavior coincides with the one found in Ref. [12] within a perturbative treatment. This trivial fixed point at the origin implies a fine tuning of the short distance physics in order to reproduce the physical scattering length. In this paper we want to extend our results for the interesting case of the triplet $^3S_1$-$^3D_1$ channel. The solution of the boundary condition problem requires solving a coupled set of Schrödinger equations. Instead of doing so, we prefer to directly compute the change of the boundary condition by an equivalent variable phase approach [37] with nontrivial initial conditions that encode the short distance physics [36].[1] This provides, in addition, a direct and quite transparent connection to renormalization group ideas [8–10]. In this paper we do not advocate any power counting in particular. Instead, we want to tackle the renormalization problem regardless of the *a priori* assumption that some perturbative expansion might work, since our formalism is flexible enough to treat any power counting.

Related works in spirit to the present one are, besides the original work of Bethe [32], the work of Ref. [11] and the more recent ones of Refs. [13,39] and [9,10]. In Ref. [32] a modified effective range expansion was defined in the context of Coulomb forces to acount for *pp* scattering (see also Ref. [11] for a more general discussion on long range potentials and higher partial waves), but assuming a regular behavior of the wave function at the origin. For those the effective range parameters are not defined, and the corresponding effective range function (M matrix) has branch cuts at small momenta. Our approach yields also a kind of modified effective range expansion, but our long range piece has a finite range $\sim 1/m_\pi$. In contrast, we can deal with singular potentials at the origin, and the analyticity of the M matrix around the origin is maintained. This is rather useful in the case of *NN* interaction since chiral potentials although exponentially suppressed at large distances become highly singular at the origin (see, e.g., Ref. [35]). In Refs. [13,39] a square well potential is used to regulate the short distance behavior simulating a smeared δ function. The renormalization group flow for the potential strength is not uniquely defined. This phenomenon is also found in the theory of self-adjoint extensions of the Schrödinger operators [42]. In Refs. [9,10] a δ shell regulator located at a finite distance is assumed as the short distance potential whereas the long distance piece is solved exactly using a distorted wave basis. This formalism has been used to the study of renormalization of repulsive singular potentials (like $1/r^2$). A common feature of both regularization schemes is that the wave function at the origin is uniquely determined by the regularity condition, $u(0) = 0$. The boundary condition regularization that we use in this paper provides a uniquely defined renormalization group flow [36], to treat both repulsive and attractive singular potentials [43]. In addition, the boundary condition admits a simple physical interpretation: it can be transformed into a variable phase shift problem [37] with a truncated potential. This interpretation directly provides the nonperturbative renormalization flow of low energy parameters and a quite transparent analysis of both infrared as well as ultraviolet fixed points and limit cycles [43].

In this paper we analyze precisely how the energy dependent boundary condition must change as we move the boundary radius for fixed energy to achieve independence of physical observables such as scattering phase shifts. By doing so we are effectively changing the Hilbert space since the wave function in the outer region is defined only from the boundary to infinity. An advantage of this procedure is that we never need to invoke off-shellness explicitly; at any step we are dealing with an on-shell problem. In addition, we work directly with finite quantities and no divergences appear at any step of the calculation when the boundary radius is taken to zero from above. Another advantage of our construction, as it will become clear along the paper, is that we only need the potentials and physical threshold parameters as input of the calculation (the cutoff dependence is removed completely, so this is not a parameter). This implies, in particular, that given this information we never have to make a fit (except perhaps for the determination of the threshold parameters); our calculations are predictions for the phase shifts that are consistent, by construction, with a low energy expansion up to a given order. Thus, the potential danger of compromising the low energy fit due to a global fit up to 300 MeV may be precluded from the start. This shows a difference with the standard way of proceeding, where the low energy parameters are fitted to the phase shifts and the threshold parameters are then recomputed. Actually, our analysis is equivalent to making a fit only in the low energy region, where explicit pions do not contribute, and predicting the intermediate energy region. We believe this is a possible and practical way of learning about the role of explicit pions

[1]For a variable phase treatment of the singlet channel with OPE and trivial boundary conditions see Ref. [38].

in the *NN* interaction. Actually, our motivation was partly to see whether OPE can actually be seen in low partial waves in the intermediate energy region $m_\pi/2 \leqslant k \leqslant m_\pi$.

In the present paper we analyze the OPE potential ($U = 2\mu V$ and $\mu = M_N/2$), which reads

$$U(\vec{x}) = U_C(r) + S_{12}U_T(r) \tag{1}$$

with ($\hat{x} = \vec{x}/r$)

$$S_{12} = 3\vec{\sigma}_1 \cdot \hat{x}\vec{\sigma}_2 \cdot \hat{x} - \vec{\sigma}_1 \cdot \vec{\sigma}_2 \tag{2}$$

and

$$U_C = -\frac{m_\pi^2 M_N g_A^2}{16\pi f_\pi^2}\frac{e^{-m_\pi r}}{r}, \tag{3}$$

$$U_T = -\frac{m_\pi^2 M_N g_A^2}{16\pi f_\pi^2}\frac{e^{-m_\pi r}}{r}\left(1 + \frac{3}{m_\pi r} + \frac{3}{(m_\pi r)^2}\right), \tag{4}$$

where M_N is the nucleon mass, m_π the pion mass, f_π the pion weak decay constant, and g_A the nucleon axial coupling constant. In the numerical calculations below we take $M_N = 938.92$ MeV, $f_\pi = 93$ MeV, $m_\pi = 138$ MeV, and $g_A = 1.25$. Note that the singularity at the origin of the tensor potential

$$U_T \to -\frac{3M_N g_A^2}{16\pi f_\pi^2 r^3} \quad r \to 0 \tag{5}$$

is independent on the pion mass m_π.

The plan of the paper is as follows. In Sec. II we present the basic object of our analysis, the variable *S*-matrix, which we supplement with general mixed boundary conditions in the general case of coupled channel scattering. We also discuss the role played by the irregular solutions for singular potentials in the spirit of an effective field theory. After that we rewrite in Sec. III the variable *S*-matrix equation for the variable *M* matrix in a way that the low energy limit may be taken. As a result, we find the boundary radius evolution of threshold parameters. We apply the resulting equations to determine the low energy threshold parameters from well established *NN* potentials, which we relegate to the Appendix. In Sec. IV we study the short distance behavior of the threshold parameters. There we show that one has for the $^1S_0$ and $^3S_1$-$^3D_1$ channels an UV fixed point and a UV limit cycle for the scattering lengths. In Sec. V we present our numerical results, both for the threshold parameters as well as for the $^1S_0$ and $^3S_1$-$^3D_1$ phase shifts. Finally in Sec. VI we present some final remarks, conclusions, and perspectives for future work.

II. VARIABLE *S* MATRIX WITH BOUNDARY CONDITIONS

In order to generalize to triplet states the results of Ref. [36] for the singlet channel case, we introduce the variable *S*-matrix formalism for the general coupled channel case. For potentials that are either regular or singular repulsive at the origin the procedure is standard [37] and it has many variants. For completeness and to make the exposition more self contained we present here our particular derivation which also applies to singular attractive potentials and at the same time introduce our basic notation for the rest of the paper. Although in the case under study we are interested in, at most, two coupled channels, the formalism can be developed for the general case with almost no additional effort.

The coupled channel Schrödinger equation for the relative motion reads

$$-\mathbf{u}''(r) + \left[\mathbf{U}(r) + \frac{\mathbf{l}^2}{r^2}\right]\mathbf{u}(r) = k^2\mathbf{u}(r), \tag{6}$$

where $\mathbf{U}(r)$ is the coupled channel matrix potential, $\mathbf{l}^2 = \mathrm{diag}(l_1(l_1+1), \ldots, l_N(l_N+1))$ is the angular momentum, $\mathbf{u}(r)$ is the reduced matrix wave function, and k is the c.m. momentum. We assume for $\mathbf{u}(r)$ the mixed boundary condition[2]

$$\mathbf{u}'(R) - \mathbf{L}_k(R)\mathbf{u}(R) = 0, \tag{7}$$

where $\mathbf{L}_k(R)$ is a real Hermitean matrix in coupled channel space, which in our framework encodes the *unknown* physics at distances r below the boundary radius R. In addition, we assume the asymptotic normalization condition

$$\mathbf{u}(r) \to \mathbf{u}_{\rm in}(r) - \mathbf{u}_{\rm out}(r)\mathbf{S}, \tag{8}$$

with $\mathbf{S}$ the standard coupled channel *S* matrix. The corresponding outgoing and ingoing free spherical waves are given by

$$\mathbf{u}_{\rm out}(r) = \mathrm{diag}(\hat{h}^+_{l_1}(kr), \ldots, \hat{h}^+_{l_N}(kr)) \equiv \mathbf{h}^{(+)}(R),$$

$$\mathbf{u}_{\rm in}(r) = \mathrm{diag}(\hat{h}^-_{l_1}(kr), \ldots, \hat{h}^-_{l_N}(kr)) \equiv \mathbf{h}^{(-)}(R), \tag{9}$$

with $\hat{h}^\pm_l(x)$ the reduced Hankel functions of order l, $\hat{h}^\pm_l(x) = xH^\pm_{l+1/2}(x)$ ($\hat{h}^\pm_0 = e^{\pm ix}$), and satisfy the free Schrödinger's equation for a free particle,

$$-\mathbf{u}''_{\rm out}(r) + \frac{\mathbf{l}^2}{r^2}\mathbf{u}_{\rm out}(r) = k^2\mathbf{u}_{\rm out}(r), \tag{10}$$

$$-\mathbf{u}''_{\rm in}(r) + \frac{\mathbf{l}^2}{r^2}\mathbf{u}_{\rm in}(r) = k^2\mathbf{u}_{\rm in}(r). \tag{11}$$

The boundary condition, Eq. (7), for the *outer* boundary value problem, Eq. (6) and Eq. (8), can be interpreted in simple physical terms of a complementary *inner* problem where the potential $\mathbf{U}(r)$ acts in the interval $R \leqslant r < \infty$. If we switch off the potential above a given boundary radius R we have, at the boundary

$$\mathbf{L}_k(R) = \mathbf{u}'(R)\mathbf{u}^{-1}(R) = [\mathbf{u}'_{\rm in}(R) - \mathbf{u}'_{\rm out}(R)\mathbf{S}(R)][\mathbf{u}_{\rm in}(R) - \mathbf{u}_{\rm out}(R)\mathbf{S}(R)]^{-1}, \tag{12}$$

where $\mathbf{S}(\mathbf{R})$ is the *S* matrix associated to the potential $\mathbf{U}(r)$ acting in the region $0 < r \leqslant R$, which inherits the dependence on the chosen boundary radius R. The equation satisfied by the variable *S* matrix can be obtained from Schrödinger's equation applied to the matrix $\mathbf{L}(R)$, yielding

[2]This is the most general boundary condition that makes the coupled channel Hamiltonian self-adjoint in the interval $R \leqslant r < \infty$.

$$\mathbf{L}_k(R)' + \mathbf{L}_k(R)^2 = \mathbf{U}(R) + \frac{\mathbf{l}^2}{R^2} - k^2. \tag{13}$$

From here[3] it is straightforward to obtain the equation for the variable S matrix,

$$2ik\frac{d\mathbf{S}(R)}{dR} = [\mathbf{S}(R)\hat{\mathbf{h}}^{(+)}(R) - \hat{\mathbf{h}}^{(-)}(R)]\mathbf{U}(R) \times [\hat{\mathbf{h}}^{(-)}(R) - \hat{\mathbf{h}}^{(+)}(R)\mathbf{S}(R)]. \tag{14}$$

This is a first order nonlinear matrix differential equation that can be solved by standard means, provided the S matrix is known at one given scale. One of the interesting aspects of this equation is that there is no need to invoke any off-shellness; for any value of the boundary radius we have a different on-shell scattering problem. As we will discuss below, Eq. (14) describes the renormalization group flow of the S matrix as a function of the distance scale R where the long range potential is truncated.

In the case of a regular potential, Eq. (14) has to be supplemented with an initial condition at the origin, namely the trivial one (corresponding to the absence of a potential), and its asymptotic value yields the full S matrix

$$\mathbf{S}(0) = 1, \quad \mathbf{S} = \mathbf{S}(\infty) \text{ (regular)}. \tag{15}$$

In this paper we are concerned with the OPE potential, which has a singular $1/r$ behavior at the origin in the ${}^1S_0$ singlet channel and singular $1/r^3$ behavior at the origin due to the tensor force in the ${}^3S_1$-${}^3D_1$ triplet channel. While in the singlet channel the singularity is a mild one in the sense that there still exists a unique regular solution at the origin, $u(0)=0$ (like in the Coulomb potential), in the triplet channel both linearly independent solutions to Schrödinger's equation vanish at the origin, and the regularity condition $u(0)=0$ does not uniquely specify the solution.

The point of view we take in the present work is that of an EFT; low energy physics should not depend on the detailed knowledge of the interaction at short distances. This applies, in particular, to the case of a singular potential as will also become clear below. Following the lines already sketched in our previous work [36], we take instead the value at infinity as the initial value for the variable S matrix. Of course, for a short range potential, this corresponds to start integration at sufficiently large distances (where the potential may be neglected). An advantage of this procedure is that *by construction* a unique solution $\mathbf{S}(R)$ is obtained. Even for a regular potential, it is clear that a generic choice of $\mathbf{S}(\infty)$ cannot yield by downward integration towards the origin the result $\mathbf{S}(0)=\mathbf{1}$ besides the very exceptional cases which accidentally correspond to the regular solution at the origin. Thus, we expect in general an admixture of both the regular and irregular solutions, which corresponds to a mixed boundary condition close to the origin,

$$\lim_{R\to 0^+}\{\mathbf{u}'(R) - \mathbf{L}(R)\mathbf{u}(R)\} = 0. \tag{16}$$

In the case of a singular potential both solutions vanish and we equally have a unique mixed boundary condition as in Eq. (16). Thus, we may define the *short distance S* matrix as the extrapolation to the origin of a given solution at infinity,

$$\mathbf{S}_s \equiv \lim_{R\to 0^+} \mathbf{S}(R), \quad \mathbf{S} = \mathbf{S}(\infty) \text{ (general)}. \tag{17}$$

Actually, the precise meaning of the previous limit will be the main topic of the present work. We anticipate already that we will find ultraviolet fixed points for the singlet ${}^1S_0$ channel and limit cycles for the ${}^3S_1$-${}^3D_1$ triplet channel. Eqs. (14) and (18) are well known in potential scattering (for a review see, e.g., Ref. [37]), but they have always been used assuming the trivial initial conditions $\mathbf{S}(0)=1$.

Obviously, if one would literally use the full S matrix and integrate downwards, nothing could be achieved, since that would correspond to eliminating the full potential. A more interesting perspective, already pursued in Ref. [36] for the singlet ${}^1S_0$ channel, consists of regarding the low energy limit of the previous equations, extracting the threshold parameters at short distances by integrating downwards from their experimental values and integrate back upwards the variable S-matrix equation to infinity. Physically, this procedure corresponds to explicitly separating the OPE contributions on top of any good low energy approximation, like, e.g., the effective range expansion.

In the case of one channel, like the ${}^1S_0$, the S matrix can be parameterized as $S_l(k,R)=\exp[2i\delta_l(k,R)]$, with $\delta_l(k,R)$ the variable phase. Equation (14) becomes rather simple [37] for s waves, yielding

$$\frac{d\delta_0(k,R)}{dR} = -\frac{1}{k}U(R)\sin^2[kR + \delta_0(k,R)], \tag{18}$$

and the obvious conditions both at the origin and at infinity must be satisfied:

$$\lim_{R\to 0}\delta_0(k,R) = \delta_0^S(k), \quad \lim_{R\to\infty}\delta_0(k,R) = \delta_0(k). \tag{19}$$

The OPE potential in the coupled triplet ${}^3S_1$-${}^3D_1$ channel space is given by

$$\mathbf{U}(r) = \begin{pmatrix} U_s(r) & U_{sd}(r) \\ U_{sd}(r) & U_d(r) \end{pmatrix}, \tag{20}$$

where

$$U_s = U_C, \quad U_{sd} = 2\sqrt{2}U_T, \quad U_d = U_C - 2U_T. \tag{21}$$

The two coupled channel S-matrix can be represented in the Blatt-Biedenharn (BB or eigen phase) parameterization:

$$S = \begin{pmatrix} \cos\epsilon & -\sin\epsilon \\ \sin\epsilon & \cos\epsilon \end{pmatrix}\begin{pmatrix} e^{2i\delta_1} & 0 \\ 0 & e^{2i\delta_2} \end{pmatrix}\begin{pmatrix} \cos\epsilon & \sin\epsilon \\ -\sin\epsilon & \cos\epsilon \end{pmatrix}, \tag{22}$$

which will be used along this paper. The relation to the coupled channel effective range function or M matrix is given by[4]

[3] An alternative derivation of Eq. (13), closer in spirit to the renormalization group and the Callan-Symanzik equation will be presented elsewhere in Ref. [43].

[4] In the one channel case $M=k\cot\delta$.

$$\mathbf{S} = (\mathbf{M} + \mathrm{i}k)(\mathbf{M} - \mathrm{i}k)^{-1}. \tag{23}$$

The low energy limit acquires its simplest form in the Stapp-Ypsilantis-Metropolis (SYM or nuclear bar) parameterization

$$S = \begin{pmatrix} e^{2\mathrm{i}\overline{\delta}_1}\cos 2\overline{\epsilon} & \mathrm{i}e^{\mathrm{i}(\overline{\delta}_1+\overline{\delta}_2)}\sin 2\overline{\epsilon} \\ \mathrm{i}e^{\mathrm{i}(\overline{\delta}_1+\overline{\delta}_2)}\sin 2\overline{\epsilon} & e^{2\mathrm{i}\overline{\delta}_2}\cos 2\overline{\epsilon} \end{pmatrix}, \tag{24}$$

which is related to the BB phase shifts by

$$\overline{\delta}_1 + \overline{\delta}_2 = \delta_+ + \delta_-, \tag{25}$$

$$\sin(\overline{\delta}_1 - \overline{\delta}_2) = \frac{\tan(2\overline{\epsilon})}{\tan(2\epsilon)}. \tag{26}$$

The low energy limit in the SYM representation becomes

$$\overline{\delta}_1 \to -\alpha_0 k, \quad \overline{\delta}_2 \to -\alpha_2 k^5, \quad \overline{\epsilon} \to -\alpha_{02} k^3 \tag{27}$$

The scaled M matrix, $\hat{\mathbf{M}}$, has a good low energy behavior and is defined [44] (see e.g. Ref. [45] for a review and many references therein) by making an energy dependent transformation

$$\hat{\mathbf{M}} = \mathbf{DMD} \tag{28}$$

with $\mathbf{D} = \mathrm{diag}(k^{l_1}, \ldots, k^{l_N})$. The scaled M matrix admits the coupled channel analog of the effective range expansion

$$\hat{\mathbf{M}} = -\mathbf{a}^{-1} + \frac{1}{2}\mathbf{r}k^2 + \mathbf{v}k^4 + \ldots, \tag{29}$$

where **a**, **r**, and **v** are the scattering length matrix, effective range, and curvature parameters, respectively.

III. EVOLUTION OF LOW ENERGY PARAMETERS

In order to take this low energy limit and corrections thereof, we introduce the variable or running M matrix

$$\mathbf{S}(R) = [\mathbf{M}(R) + \mathrm{i}k][\mathbf{M}(R) - \mathrm{i}k]^{-1} \tag{30}$$

as well as the reduced Bessel functions

$$\hat{j}_l(x) = x j_l(x), \quad \hat{y}_l(x) = x y_l(x), \tag{31}$$

i.e., $\hat{j}_0(x) = \sin x$, $\hat{y}_0(x) = -\cos x$. Thus,

$$\hat{\mathbf{j}} = \frac{1}{2\mathrm{i}}(\hat{\mathbf{h}}^{(+)} - \hat{\mathbf{h}}^{(-)}), \tag{32}$$

$$-\hat{\mathbf{y}} = \frac{1}{2}(\hat{\mathbf{h}}^{(+)} + \hat{\mathbf{h}}^{(-)}). \tag{33}$$

Then we get

$$\mathbf{M}'(k,R) = \left(\frac{1}{k}\mathbf{M}(k,R)\hat{\mathbf{j}}(kR) - \hat{\mathbf{y}}(kR)\right)\mathbf{U}(R) \times \left(\frac{1}{k}\hat{\mathbf{j}}(kR)\mathbf{M}(k,R) - \hat{\mathbf{y}}(kR)\right). \tag{34}$$

The running scaled M matrix, $\hat{\mathbf{M}}(R)$, is defined similarly to Eq. (28),

$$\hat{\mathbf{M}}(R) = \mathbf{DM}(R)\mathbf{D} \tag{35}$$

and satisfies the equation

$$\hat{\mathbf{M}}'(k,R) = \left(\hat{\mathbf{M}}(R,k)\frac{1}{k}\mathbf{j}(kR)\mathbf{D}^{-1} - \mathbf{y}(kR)\mathbf{D}\right)\mathbf{U}(R) \times \left(\frac{1}{k}\mathbf{j}(kR)\mathbf{D}^{-1}\hat{\mathbf{M}}(R,k) - \mathbf{y}(kR)\mathbf{D}\right). \tag{36}$$

The scaled M matrix admits the analog of the effective range expansion

$$\hat{\mathbf{M}}(R) = -\mathbf{a}(R)^{-1} + \frac{1}{2}\mathbf{r}(R)k^2 + \mathbf{v}(R)k^4 + \cdots, \tag{37}$$

where $\mathbf{a}(R)$, $\mathbf{r}(R)$, and $\mathbf{v}(R)$ are the corresponding running scattering length matrix, effective range, and curvature parameters, respectively. In this form the low energy limit can be easily taken. Defining the matrix functions and their low energy expansion

$$\mathbf{A}_k(R) = \frac{\mathbf{j}(kR)}{k}\mathbf{D}^{-1} = \mathbf{A}_0 + k^2\mathbf{A}_2 + k^4\mathbf{A}_4 + \ldots, \tag{38}$$

$$\mathbf{B}_k(R) = \mathbf{y}(kR)\mathbf{D} = \mathbf{B}_0 + k^2\mathbf{B}_2 + k^4\mathbf{B}_4 + \ldots, \tag{39}$$

we get the system of coupled equations

$$\frac{d}{dR}[\mathbf{a}(R)]^{-1} = -\{[\mathbf{a}(R)]^{-1}\mathbf{A}_0 + \mathbf{B}_0\}\mathbf{U}(R)\{\mathbf{A}_0[\mathbf{a}(R)]^{-1} + \mathbf{B}_0\},$$

$$\frac{d}{dR}\mathbf{r}(R) = \{[\mathbf{a}(R)]^{-1}\mathbf{A}_0 + \mathbf{B}_0\}\mathbf{U}(R)\{\mathbf{r}(R)\mathbf{A}_0 + 2[\mathbf{a}(R)]^{-1}\mathbf{A}_2 + 2\mathbf{B}_2\} + \{\mathbf{r}(R)\mathbf{A}_0 + 2[\mathbf{a}(R)]^{-1}\mathbf{A}_2 + 2\mathbf{B}_2\}\mathbf{U}(R) \times\{[\mathbf{a}(R)]^{-1}\mathbf{A}_0 + \mathbf{B}_0\},$$

$$\frac{d}{dR}\mathbf{v}(R) = ([\mathbf{a}(R)]^{-1}\mathbf{A}_0 + \mathbf{B}_0)\mathbf{U}(R)\Big\{-[\mathbf{a}(R)]^{-1}\mathbf{A}_4 + \tfrac{1}{2}\mathbf{r}(R)\mathbf{A}_2 + \mathbf{v}(R)\mathbf{A}_0 - \mathbf{B}_4\Big\} + \Big\{-[\mathbf{a}(R)]^{-1}\mathbf{A}_4 + \tfrac{1}{2}\mathbf{r}(R)\mathbf{A}_2 + \mathbf{v}(R)\mathbf{A}_0 - \mathbf{B}_4\Big\}\mathbf{U}(R)\{[\mathbf{a}(R)]^{-1}\mathbf{A}_0 + \mathbf{B}_0\} + \Big\{\tfrac{1}{2}\mathbf{r}(R)\mathbf{A}_2 - [\mathbf{a}(R)]^{-1}\mathbf{A}_2 - \mathbf{B}_2\Big\}\mathbf{U}(R)\Big\{\tfrac{1}{2}\mathbf{r}(R)\mathbf{A}_2 - [\mathbf{a}(R)]^{-1}\mathbf{A}_2 - \mathbf{B}_2\Big\}. \tag{40}$$

These equations generalize to the coupled channel case those already found in Ref. [36] and have to be supplemented with some initial conditions, at, e.g., infinity,

$$\mathbf{a}(\infty) = \mathbf{a}, \quad \mathbf{r}(\infty) = \mathbf{r}, \quad \mathbf{v}(\infty) = \mathbf{v}. \tag{41}$$

For the case of s wave one channel scattering Eq. (36) becomes

$$\frac{dM(k,R)}{dR} = U(R)\left[M(k,R)\frac{\sin kR}{k} + \cos kR\right]^2, \tag{42}$$

where

$$M(k,R) = k\cot\delta(k,R), \tag{43}$$

yielding at low energies an effective range expansion,

$$k\cot\delta(k,R) = -\frac{1}{\alpha_0(R)} + \frac{1}{2}r_0(R)k^2 + v_2(R)k^3\cdots \quad (44)$$

where

$$\frac{d\alpha_0}{dR} = U(R)(\alpha_0 - R)^2, \quad (45)$$

$$\frac{dr_0}{dR} = 2U(R)R^2\left(1-\frac{R}{\alpha_0}\right)\left(\frac{r_0}{R}+\frac{R}{3\alpha_0}-1\right), \quad (46)$$

$$\frac{dv_2}{dR} = \frac{U(R)}{R}\left\{\frac{1}{4}\left(\frac{r_0}{R}+\frac{R}{3\alpha_0}-1\right)^2 + 2\left(1-\frac{R}{\alpha_0}\right)\left(-\frac{1}{12}\frac{r_0}{R}+\frac{v_2}{R^3} - \frac{1}{120}\frac{R}{\alpha_0}+\frac{1}{24}\right)\right\}. \quad (47)$$

These equations have been studied by us in Ref. [36] for analyzing the OPE in the singlet $^1S_0$ channel.

In the $^3S_1$-$^3D_1$ coupled channel case the threshold parameters matrices are

$$\mathbf{a} = \begin{pmatrix} \alpha_0 & \alpha_{02} \\ \alpha_{02} & \alpha_2 \end{pmatrix}, \quad (48)$$

$$\mathbf{r} = \begin{pmatrix} r_0 & r_{02} \\ r_{02} & r_2 \end{pmatrix}, \quad (49)$$

$$\mathbf{v} = \begin{pmatrix} v_0 & v_{02} \\ v_{02} & v_2 \end{pmatrix}. \quad (50)$$

The explicit form of the equations for the $^3S_1$-$^3D_1$ running scattering lengths reads

$$R^4\alpha_0' = 9U_d\alpha_{02}^2 + (\alpha_0 - R)R^2[(\alpha_0 - R)U_s + 6\alpha_{02}U_{sd}],$$

$$15R^5\alpha_{02}' = -15\alpha_{02}R^4(-\alpha_0 + R)U_s + R^2[45\alpha_{02}^2 - (\alpha_0 - R) \times(-45\alpha_2 + R^5)]U_{sd} - 3\alpha_{02}(-45\alpha_2 + R^5)U_d,$$

$$225R^4\alpha_2' = 225\alpha_{02}^2R^4U_s - 30\alpha_{02}R^2(-45\alpha_2 + R^5)U_{sd} + (-45\alpha_2 + R^5)^2U_d. \quad (51)$$

Note that all three running low energy parameters α_0, α_{02}, and α_2 (the explicit R-dependence has been suppressed for simplicity) are coupled due to the mixing potential U_{sd}. Thus, it would be inconsistent to take any of them as a constant; exact renormalization group invariance requires mixing between the S and D channels. As we see the mixing is related both to a nonvanishing of the mixing potential U_{sd} and a nonvanishing value of α_{sd} at a given point. If by some accident both vanish at a given point, the mixing will vanish.

The evolution of the low energy parameters can be translated into the corresponding evolution of the short distance boundary condition as a function of the boundary radius. Defining the dimensionless quantity

$$\mathbf{C}_k(R) = \mathbf{1} - R\mathbf{L}_k(R) = \mathbf{1} - R\mathbf{u}_k'(R)\mathbf{u}_k(R)^{-1} \quad (52)$$

and using Eq. (13) we get

$$-R\mathbf{C}_k'(R) = \mathbf{C}_\mathbf{k}(\mathbf{1} - \mathbf{C}_\mathbf{k}) + \mathbf{U}(R)R^2 + \mathbf{l}^2 - k^2R^2. \quad (53)$$

Expanding into powers of the momentum k one gets

$$\mathbf{C}_k(R) = \mathbf{C}_0(R) + k^2R^2\mathbf{C}_2(R) + \cdots. \quad (54)$$

For the singlet $^1S_0$ channel we have, in particular,

$$C_0 = \frac{\alpha_0(R)}{R - \alpha_0(R)}. \quad (55)$$

Note that for $R\to\infty$ we have a fixed point behavior $C_0\to 0$ unless $\alpha=\infty$ in which case $C_0\to 1$. The evolution of the boundary condition with the short distance boundary radius for $^3S_1$-$^3D_1$ in terms of the running scattering lengths is given by

$$C_s^0 = 1 + \frac{R(R^5 - 45\alpha_{22})}{45\alpha_{02}^2 + (\alpha_{00} - R)(R^5 - 45\alpha_{22})}, \quad (56)$$

$$C_{sd}^0 = \frac{15\alpha_{02}R^3}{45\alpha_{02}^2 + (\alpha_{00} - R)(R^5 - 45\alpha_{22})}, \quad (57)$$

$$C_d^0 = 3 - \frac{5(R - \alpha_{00})R^5}{45\alpha_{02}^2 + (\alpha_{00} - R)(R^5 - 45\alpha_{22})}. \quad (58)$$

Again, for $R\to\infty$ we have for nonexceptional values of the parameters $C_s^0\to 0$, $C_{sd}^0\to 0$, and $C_d^0\to -2$. In Ref. [43] a more detailed study on these issues will be carried out.

IV. SHORT DISTANCE BEHAVIOR FOR OPE: FIXED POINTS AND LIMIT CYCLES

In this section we analyze the short distance behavior of the equations for the scattering lengths for the singlet $^1S_0$, Eq. (45), and the triplet $^3S_1$-$^3D_1$, Eq. (51), channels in the short distance limit. According to Eq. (12) this is equivalent to study the mixed boundary condition at short distances.

We study first the case of OPE in the singlet $^1S_0$ channel. At short distances $R \ll 1/m_\pi$ the OPE potential behaves like the Coulomb potential. Equation (45) can be easily solved in two extreme cases, $\alpha_0 \ll R$ and $\alpha_0 \gg R$. While in the first case we get

$$\alpha_0(R) \to -\frac{g_A^2m_\pi^2M_N}{32\pi f_\pi^2}R^2,\ \alpha_0 \ll R \quad (59)$$

in the second case one solution behaves as

$$\alpha_0(R) \to \frac{16\pi f_\pi^2}{g_A^2m_\pi^2M_N}\frac{1}{\log(R/R_0)},\ \alpha_0 \ll R \quad (60)$$

where R_0 is a reference scale fulfilling $R < R_0 \ll 1/m_\pi$. As we see, $\alpha_0(R)$ goes to zero in both cases but, while Eq. (59) goes rapidly $\alpha_0'(R)\to 0$, Eq. (60) goes very slowly and with $\alpha_0'(R)\to -\infty$ at short distances. In momentum space the $R\to 0$ limit corresponds to the ultraviolet limit. Equation (60) resembles a sort of asymptotic freedom and hence we have an ultraviolet fixed point. One can see that the first case, Eq. (59), corresponds to selecting the regular solution at the origin, whereas Eq. (60) corresponds to a generic case, which

always contains an admixture of the irregular solution. The regular case at the origin corresponds to integrate from the origin starting with the trivial initial condition $\delta(k,0)=0$ up to infinity. As we have discussed in Ref. [36] the result corresponds to a pure OPE interaction, with no short distance interactions. The important thing to realize is that regardless of the value of α_0 at infinity, removing one-pion exchange goes into the same value at the origin, as implied by Eq. (60). This also implies that any tiny deviation of the $\alpha_0(R)$ at small distances results in huge variations at infinity. Thus, removing OPE in the ${}^1S_0$ channel implies an extreme fine tuning of the scattering length at short distances, and hence of the boundary condition at the origin.

We turn now to the case of the ${}^3S_1$-${}^3D_1$ channel, where the tensor force plays a role. In the region close to the origin the wave function oscillates wildly and hence a WKB approximation may be used. The calculation is simplified by taking into account that for the OPE interaction the potential matrix is diagonalized by an r-independent unitary transformation, i.e.,

$$\mathbf{M}\mathbf{U}(r)\mathbf{M}^{-1}=\begin{pmatrix} U_C(r)-4U_T(r) & 0 \\ 0 & U_C(r)+2U_T(r) \end{pmatrix}, \tag{61}$$

with

$$\mathbf{M}=\begin{pmatrix} -\frac{1}{\sqrt{2}} & 1 \\ \sqrt{2} & 1 \end{pmatrix}. \tag{62}$$

Note that this transformation *does not* diagonalize the full potential $\mathbf{U}+\mathbf{l}^2/r^2$ including the centrifugal barrier, which for $r\to 0$ may be neglected. Thus, in the short distance limit we may decouple all our equations into pairs, and in particular we can apply the transformation to the boundary condition, Eq. (7), at zero energy

$$\mathbf{M}\mathbf{L}_0(R)\mathbf{M}^{-1}=\mathrm{diag}(l_1(R),l_2(R)), \tag{63}$$

where $l_1(R)$ and $l_2(R)$ are the logarithmic derivatives at zero energy of the decoupled problem with potentials $U_1=U_C-4U_T$ and $U_2=U_C+2U_T$, respectively. After straightforward algebra we get

$$\alpha_0(R)=3\frac{Rl_2(R)(Rl_1(R)+1)-2}{4l_2(R)+l_1(R)(3Rl_2(R)+2)}, \tag{64}$$

$$\alpha_{02}(R)=-\frac{\sqrt{2}R^3}{3}\frac{l_1(R)-l_2(R)}{4l_2(R)+l_1(R)(3Rl_2(R)+2)}, \tag{65}$$

$$\alpha_2(R)=\frac{R^5}{15}\frac{l_1(R)(Rl_2(R)-1)-2l_2(R)}{4l_2(R)+l_1(R)(3Rl_2(R)+2)}. \tag{66}$$

Now, as we approach the origin the tensor potential dominates, and the potentials U_1 and U_2 behave as repulsive and attractive $1/r^3$ potentials, respectively, corresponding to taking $l_1\to\infty$ and $l_2(R)$ by the zero energy limit of the logarithmic derivative of a WKB function,

$$\alpha_0(R)\to R\frac{3Rl_{\mathrm{WKB}}(R)}{3Rl_{\mathrm{WKB}}(R)+2}, \tag{67}$$

$$\alpha_{02}(R)\to-\frac{\sqrt{2}R^3}{3}\frac{1}{3Rl_{\mathrm{WKB}}(R)+2}, \tag{68}$$

$$\alpha_2(R)\to\frac{R^5}{15}\frac{Rl_{\mathrm{WKB}}(R)-1}{3Rl_{\mathrm{WKB}}(R)+2}, \tag{69}$$

with

$$Rl_{\mathrm{WKB}}(R)=\frac{3}{4}+\frac{1}{2}\sqrt{\frac{R_M}{R}}\cot\left(\Delta+\left[\sqrt{\frac{R_M}{R_0}}-\sqrt{\frac{R_M}{R}}\right]\right). \tag{70}$$

Here Δ is an energy independent phase, and R_0 a reference point, given by

$$R_0l_{\mathrm{WKB}}(R_0)=\frac{3}{4}+\frac{1}{2}\sqrt{\frac{R_M}{R_0}}\cot(\Delta) \tag{71}$$

and

$$R_M=\frac{3g^2M}{2f^2\pi}=16\ \mathrm{fm}. \tag{72}$$

As we see the scattering lengths α_0, α_{02}, and α_2 present an oscillatory behavior as we approach the origin, so they do not converge to a well defined value; as we approach the origin the α's take all possible values. This situation corresponds to a limit cycle at short distances.[5] A way of avoiding the unbound variation of the scattering lengths consists of going to the origin stepwise through some envelope subsequence defined by a fixed condition for $l_{\mathrm{WKB}}(R)$. For instance, if we define a cycle by the condition $\alpha(R_n)=0$, we have $R_nl_{\mathrm{WKB}}(R_n)=0$, yielding

[5]We use the term limit cycle in a loose sense as already done in Ref. [39]. These are to be distinguished from the limit cycles obtained for an attractive $1/r^2$ potential (see, e.g., Refs. [40,41] and references therein for a discussion on the context of Efimov states in the three body problem) where a logarithmic flow with the regulator scale is found. This behavior can trivially be seen from the evolution of the dimensionless boundary condition C_0 from Eq. (53) [see also Eq. 14 of Ref. [36]] in the one channel s-wave case at zero energy. For $U=g/r^2$ one has

$$-RC_0'(R)=C_0(R)[1-C_0(R)]+g, \tag{73}$$

which formally presents scale invariance explicitly broken by a nontrivial initial condition $C_0(R_0)$. This equation exhibits real and complex fixed points for $g>-1/4$ and $g<-1/4$, respectively. The latter case corresponds indeed to scale independent ultraviolet limit cycles. For more singular potentials the flow becomes "accelerated," and hence the cycles become scale dependent, although the cyclic pattern in the limit $R\to 0$ remains [43] and hence the short distance fine tuning becomes more acute.

$$\alpha_0(R_n) = 0, \tag{74}$$

$$\alpha_{02}(R_n) = -\frac{\sqrt{2}R_n^3}{6}, \tag{75}$$

$$\alpha_2(R_n) = -\frac{R_n^5}{30}. \tag{76}$$

Another possibility would be to take $l_{\rm WKB}(R_n)=\infty$, etc. As we see, there are infinitely many such possibilities, although all of them go towards the trivial values, $\alpha_0(0^+)=\alpha_{02}(0^+)=\alpha_2(0^+)=0$. Actually, any of the choices correspond to a different starting condition at infinity, modulo a cycle. Conversely, if we go to very short distances, where the scattering lengths vary wildly, any tiny perturbation there results in a completely different value at infinity. So, we see again that an extreme fine tuning of the threshold parameters at short distances is required.

In practical numerical calculations the finite integration step ΔR provides a given resolution scale, and these infinite limit cycles may not be observed due to the rapid oscillations. Instead, one sees the envelope corresponding to the stationary points of the scattering lengths. This point will become clear below, Sec. V.

V. NONPERTURBATIVE SOLUTIONS

A. Evolution of the low energy parameters

The exact mathematical analysis of the general set of equations is rather complicated since we are dealing with a nonlinear system of equations. In Ref. [43] simple cases are analyzed analytically and the general features that can be deduced there are consistent with the numerical results we have obtained in the present work.

As we have said the set of equations, Eq. (45) and Eq. (51), can be numerically solved. Given the fact that as we approach the origin the tensor part of the potential develops a singularity it is important to carefully check for numerical accuracy at short distances. A crucial property that must be fulfilled by any algorithm is that of exact reversibility; i.e., evolving upwards or downwards should be inverse operations of each other. This is a stringent test and, moreover, the only way to make sure that when the long range piece of the potential is switched on for the M-matrix integration we have consistency with the effective range expansion up to the relevant order (see also below). We prefer to impose this reversibility exactly, independently, on the number of mesh points used in the integration, so that any numerical irreversibility is merely attributable to computer arithmetic round-off errors. This feature will prove extremely relevant when computing the phase shifts below since our calculation requires upwards integration from lower distances. In all calculations presented in this paper we have checked that the correct threshold behavior is obtained. Quite generally, we find stable results when we take the long distance cutoff to be $R_\infty=20$ fm. On the other hand, the lowest radius we can achieve numerically and preserving reversibility is $R_S=0.1$ fm, mainly due to computer arithmetic round-off errors triggered by the singularity of the potential. One could further lower the radius by a semiclassical approximation as outlined in Sec. IV since as the origin is approached the wave function undergoes an increasing number of oscillations and WKB methods can be applied. Nevertheless, as we will see below, for our short distance cutoff the phase shifts for c.m. momenta up to $k=250$ MeV are rather stable numerically.

The strong dependence of the low energy threshold parameters on the short distance cutoff provides a clue to the fact that there seems to be a lower finite limit for the boundary radius $R_S=R_{\rm min}\sim 1.4$ fm [35] with still an acceptable fit; if the boundary radius is lowered, the parameters encoding the short distance boundary condition that are used as fitting parameters depend in a nonsmooth way on R_S. In addition, the strong singularity at the origin triggers a fine tuning in those parameters. According to our previous discussion, this short distance fine tuning of low energy parameters is absolutely necessary to comply with the independence of the scattering amplitude on the short distance boundary radius. For such a situation, a fit based on successive adiabatic changes of R_S becomes impractical since the fitting parameters do not change adiabatically and also because these parameters should have to be determined to extraordinary high precision. In addition, the way how the limit $R_S\to 0$ should be taken differs from channel to channel. Our method provides a practical way to overcome the difficulty, given the fact that the boundary radius is taken exactly to zero along the renormalization trajectories while keeping the low energy threshold parameters at fixed values.

1. $^1S_0$ and $^3S_1$ without mixing channels

In Fig. 1 we show our results for the evolution of the threshold parameters α_0, r_0, and v_2 in the singlet $^1S_0$ and triplet $^3S_1$ without mixing (i.e., neglecting the tensor force) channels. The main difference one can appreciate from the comparison of both channels is that while the scattering length for the $^1S_0$ channel exhibits a monotonic trend towards the origin, the scattering length in the $^3S_1$ channel diverges at a distance of about 0.7 fm. The interpretation of this fact in our framework is clear; the central part of the OPE potential is purely attractive. Thus, by eliminating the pions down to a certain distance, we are effectively building some repulsion, until we lose a bound state. An alternative interpretation is that as we switch on the OPE potential from the origin up to a certain distance we can accommodate a bound state above 0.7 fm. With this interpretation in mind, we should add 180° to the $^3S_1$ phase shift to comply with Levinson's theorem.

2. $^3S_1$-$^3D_1$ channel

We finally analyze the triplet $^3S_1$-$^3D_1$ channel taking into account the tensor mixing. In Fig. 2 we show our numerical

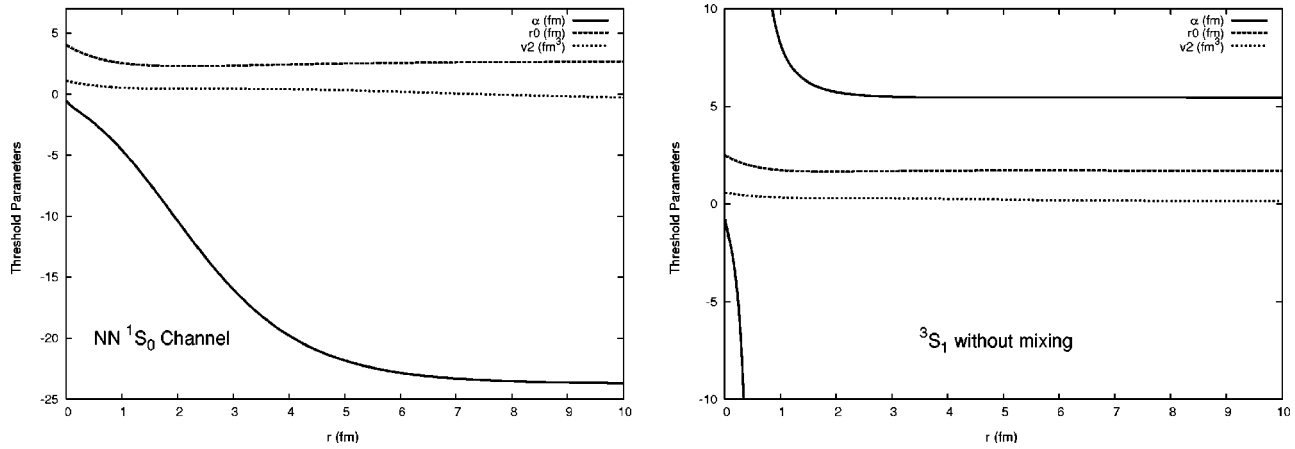

FIG. 1. Evolution of the scattering ${}^1S_0$ (left panel) and ${}^3S_1$ without mixing (right panel) *NN* threshold parameters $\alpha_0(R)$ (in fm), $r_0(R)$ (in fm), and $v_2(R)$ (in fm^3) from the asymptotic values at infinity (which we take in practice $R_\infty=20$ fm) when OPE effects are removed down to the origin.

solutions of the set of Eqs. (40), starting at sufficiently long distances (in practice $R_\infty=20$ fm turns out to be adequate) and evolving downwards to the origin. Operationally this corresponds to eliminate OPE in the triplet channel. We have clearly seen for distances above $R\sim 3$ fm nothing dramatic happens and a monotonic trend is observed. At smaller distances ~ 2 fm, however, we note a rapid change in the running scattering lengths. Again, a rather flat evolution follows until the region below 1 fm. An enlargement is plotted in Fig. 2. The number of cycles increases without any bound as the origin is approached. This situation is dramatically different from that found in the case without tensor mixing, since there OPE produced an ultraviolet fixed point. The situation we encounter here is not new and has already been described in the context of noncoupled channels. The limit cycle structure naturally raises the problem of undefined values of the short distance parameters as we take the limit $R\to 0$. The point is that there is a way of taking the limit through equivalent points defined by the property $\alpha(R_n)=\alpha(R_{n+1})$; any two such points produce identical low energy parameters at infinity. Thus, the limit $R_n\to\infty$ through equivalent points produces the same parameters at long distances. The cycles in α_{02} and α_2 are hardly seen in the plot due to a low resolution ΔR compared with the typical cycle spacing.

B. Phase shifts

The standard way of proceeding would be to determine the low energy constants or, equivalently, the short distance parameters directly from a fit to the data in a large energy range (say up to $k\sim m_\pi$ where the two-pion exchange left cut should start contributing) for the theory with OPE. The low energy parameters would have to be recomputed, and the description at lower energies ($k<m_\pi$) might become even worse than a pure effective range expansion (see, e.g., Refs. [46,47]). Obviously, this is an undesirable situation. The effective range expansion is convergent up to the OPE left cut, located at $k=\pm i m_\pi/2$, and should be applied only there.[6] Our formalism can be specifically constructed to avoid such a situation. Once the threshold parameters are determined in the short distance limit $R_S\to 0$, our phase shifts become pure predictions *without any additional parameter fitting* obtained to a given order k^2 expansion of the initial condition by integrating Eq. (42) using the effective range type of initial condition,

$$\hat{\mathbf{M}}_S=\hat{\mathbf{M}}(R_S)=-\mathbf{a}_S^{-1}+\frac{1}{2}\mathbf{r}_S k^2+\mathbf{v}_S k^4+\cdots \qquad (77)$$

with $R_S\to 0$. The solution of Eq. (42) at $R\to\infty$ gives a solution, which when expanded in powers of k^2, exactly reproduces ERE to the order imposed by the initial condition, Eq. (29). Thus, the difference beyond the displayed terms is merely attributable to the OPE potential. In what follows we use LO, NLO, NNLO, etc., to denote keeping up to the first, second, third order terms in Eq. (77), respectively.

1. ${}^1S_0$ and ${}^3S_1$ without mixing channels

In Fig. 3 we show the results for the phase shifts for both ${}^1S_0$ and ${}^3S_1$ without mixing channels depending on the number of terms kept in the low energy expansion at short distances. Our results exhibit a good convergence rate. For comparison we also depict the effective range expansion results without explicit pions, which is expected to work at low energies only. As we see, the effect of introducing pions always improves the results. This can be fully appreciated at NNLO, where ERE does a poor job above c.m. momenta ~ 100 MeV, but explicit OPE effects enlarge the energy

[6]The fact that only two terms in the expansion, involving the scattering length and the effective range only, works so well at high momenta, almost up to $k\sim m_\pi$, is purely accidental. Actually, including the next v_2 term in the expansion and fitting it in the region $k<m_\pi/2$ does not reproduce the data for $m_\pi/2<k<m_\pi$, but improves the fit for $k<m_\pi/2$. This is obviously an indication of the breakdown of the expansion beyond the analyticity domain.

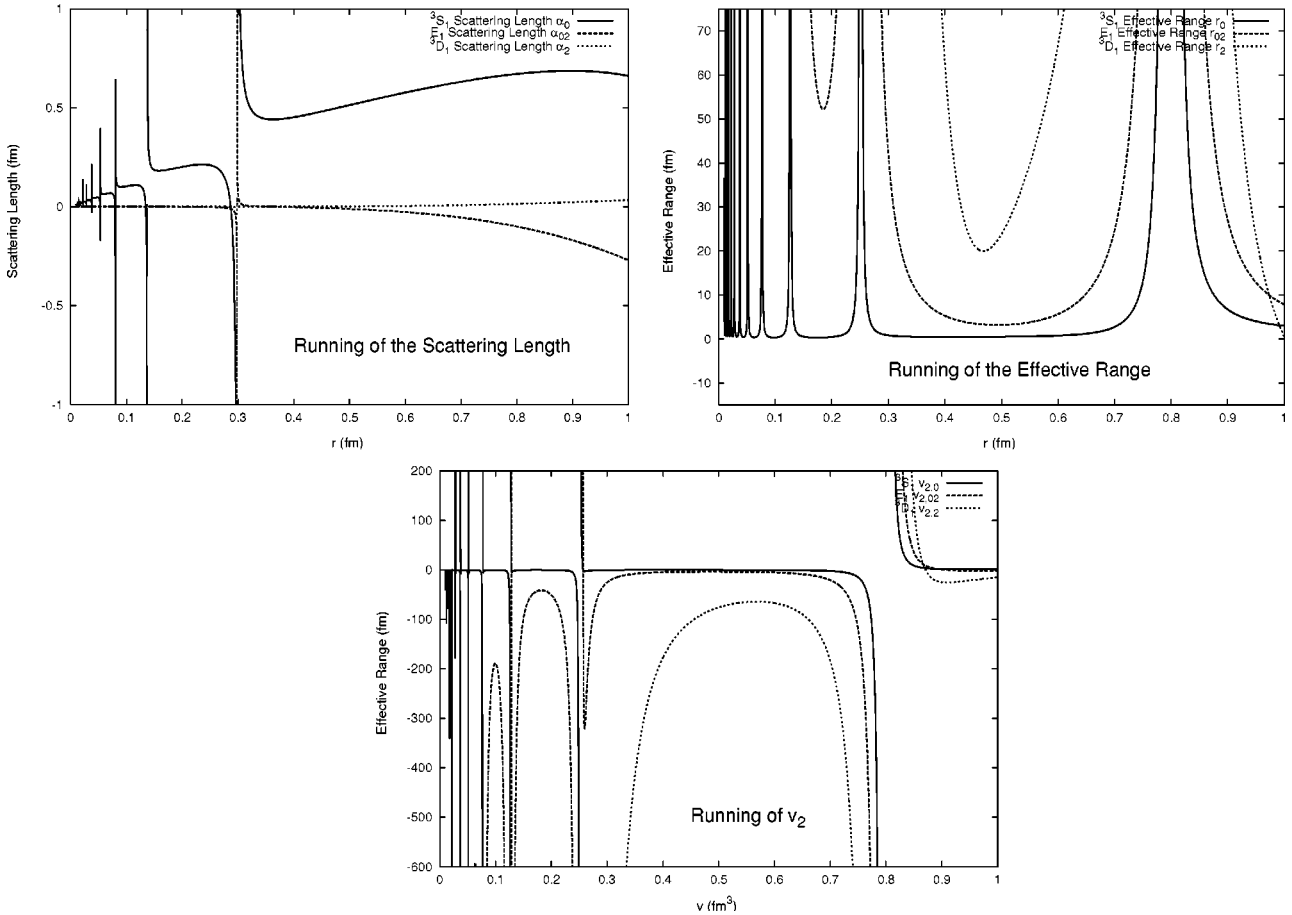

FIG. 2. Evolution of the $^3S_1$, $^3D_1$, and E_1 *NN*-threshold parameters from the physical values at infinity down to the origin using the OPE potential in the short distance region below 1 fm. Scattering lengths $\alpha_0(R)$ (in fm), $\alpha_{02}(R)$ (in fm^3), and $\alpha_2(R)$ (in fm^5). Effective ranges $r_0(R)$ (in fm), $r_{02}(R)$ (in fm^3), and $r_2(R)$ (in fm^5). Curvature parameters $v_0(R)$ (in fm^3), $v_{02}(R)$ (in fm^5), and $v_2(R)$ (in fm^7). Limit cycles are clearly visible in the *s*-wave scattering length α_0 and effective ranges. The E_1 and $^3D_1$ scattering lengths α_{02} and α_2 go quickly to zero below 0.25 fm.

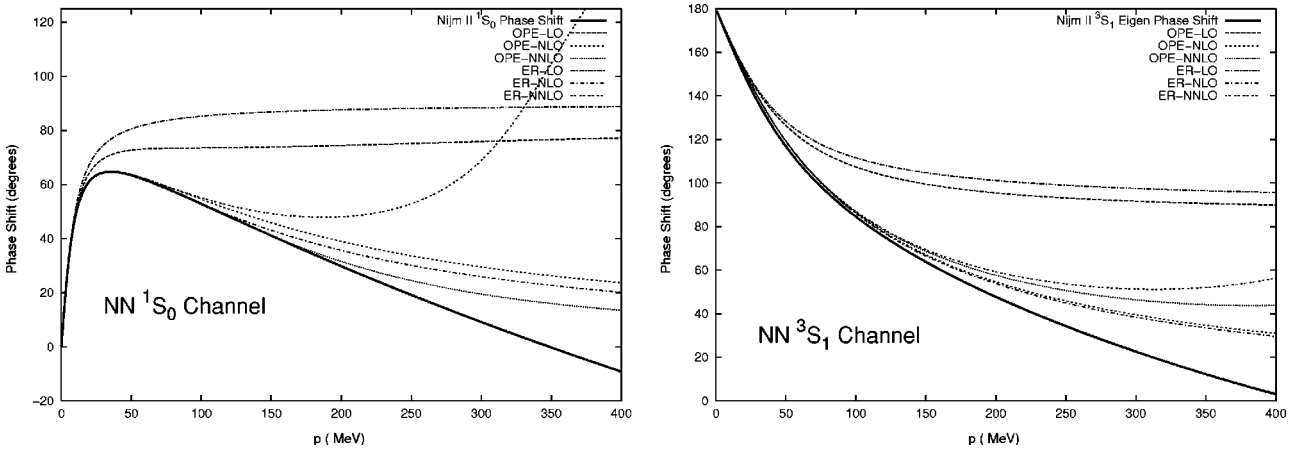

FIG. 3. Predicted phase shifts in the $^1S_0$ (left panel) and the $^3S_1$ without mixing (right panel) channels for *NN* scattering as a function of the c.m. momentum in MeV. In the $^3S_1$ channel we assume no mixing according to Eq. (42) when OPE potential is switched on and the initial condition is a low energy expansion of the *M* matrix at short distances [see Eq. (77)]. LO means keeping $\alpha_{S,0}$ only, NLO keeping $\alpha_{S,0}$ and $r_{0,S}$, and NNLO keeping $\alpha_{S,0}$, $r_{0,S}$, and $v_{2,S}$. The short range parameters are directly determined by evolving the low energy parameters from their experimental values, Eqs. (A1) and (A2), ER-LO, ER-NLO, and ER-NNLO corresponds to a pure effective range expansion keeping α_0 only, $\alpha_{S,0}$ and r_0, and α_0, r_0, and v_2, respectively. No further fit is involved. Data are the PWA from Refs. [33,34].

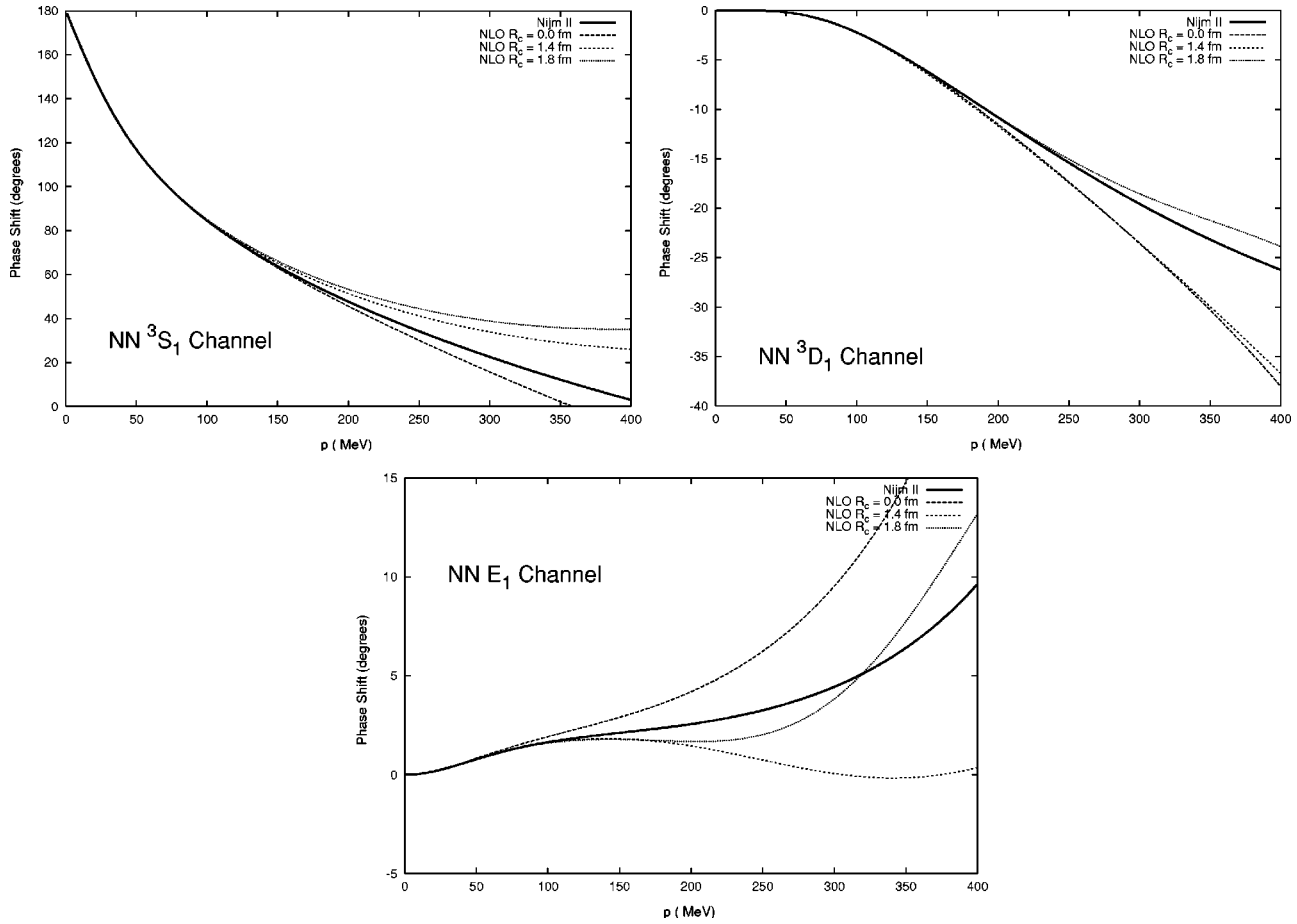

FIG. 4. The effect of having a finite short distance boundary radius for the OPE potential on top of the effective range expansion (ERE). We compare the theory with finite radii $R=1.4$ fm and $R=1.8$ fm with the renormalized theory $R=0$. We only show the results for OPE-NLO for $^3S_1$, $^3D_1$, and E_1 channels. The low energy threshold parameters coincide with those extracted from the NijmII potential. Data are the PWA from Refs. [33,34].

range up to about ~ 140 MeV$\sim m_\pi$, where we expect explicit two-pion exchange contributions to start playing a role.

2. $^3S_1$-$^3D_1$ *channel*

Once the short distance evolution of the low energy parameters are known one may compute the phase shifts to any order of the approximation in a k^2 expansion of the initial condition *without any additional parameter fitting* by integrating Eq. (42) upwards with a suitable initial condition at a short distance radius. As a matter of fact the practical choice of the radius in the numerical calculation is far from obvious, particularly in the triplet channel case where the low energy parameters take unbounded values in an increasingly finer scale at short distances (see, e.g., Fig. 2). It is most practical to use the WKB approximation to match the numerical solution at a radius $R_{\rm WKB}$, which can safely be taken in the range ~ 0.5 fm. The results for LO (contact terms), NLO (k^2 terms), and NNLO (k^4 terms) are presented in Fig. 5 and compared to the partial wave analysis (PWA) of Refs. [33,34]. As we see the best scheme to take into account the OPE potential corresponds to using the NLO initial condition. This means on the one hand that while the scattering lengths may be considered large and comparable to the effective ranges the curvature parameters v_2 can be considered to be small.

C. Finite cutoff effects

Finite short distance cutoff effects in the scattering phase shifts can be seen in Fig. 4 for finite representative radii $R_S=1.4$ fm and $R_S=1.8$ fm as compared to the renormalized $R_S=0$ case, for the OPE-NLO approximation (the OPE-LO and OPE-NNLO display similar features). As one naively expects these finite effects increase for larger energies, since they probe smaller wavelengths. A very important feature that can be deduced from the plots is that these effects are sizable for momenta where TPE effects should not play a decisive role, $m_\pi/2<k<m_\pi$. Thus, letting a finite short distance boundary radius $R_S\sim 1.4$ fm provides a large systematic error, already in the region where OPE dominates. Thus, it is not clear whether TPE can be *seen* in the central *NN* waves with a finite cutoff distance of about $R_c=1.4$ fm. Of course, one should include TPE contributions in order to make a definite statement. In any case, it is worth mentioning that the error band that would be generated by decreasing smoothly the short distance cutoff radius R_S does not follow a monotonic trend, as one might naively expect, i.e., small

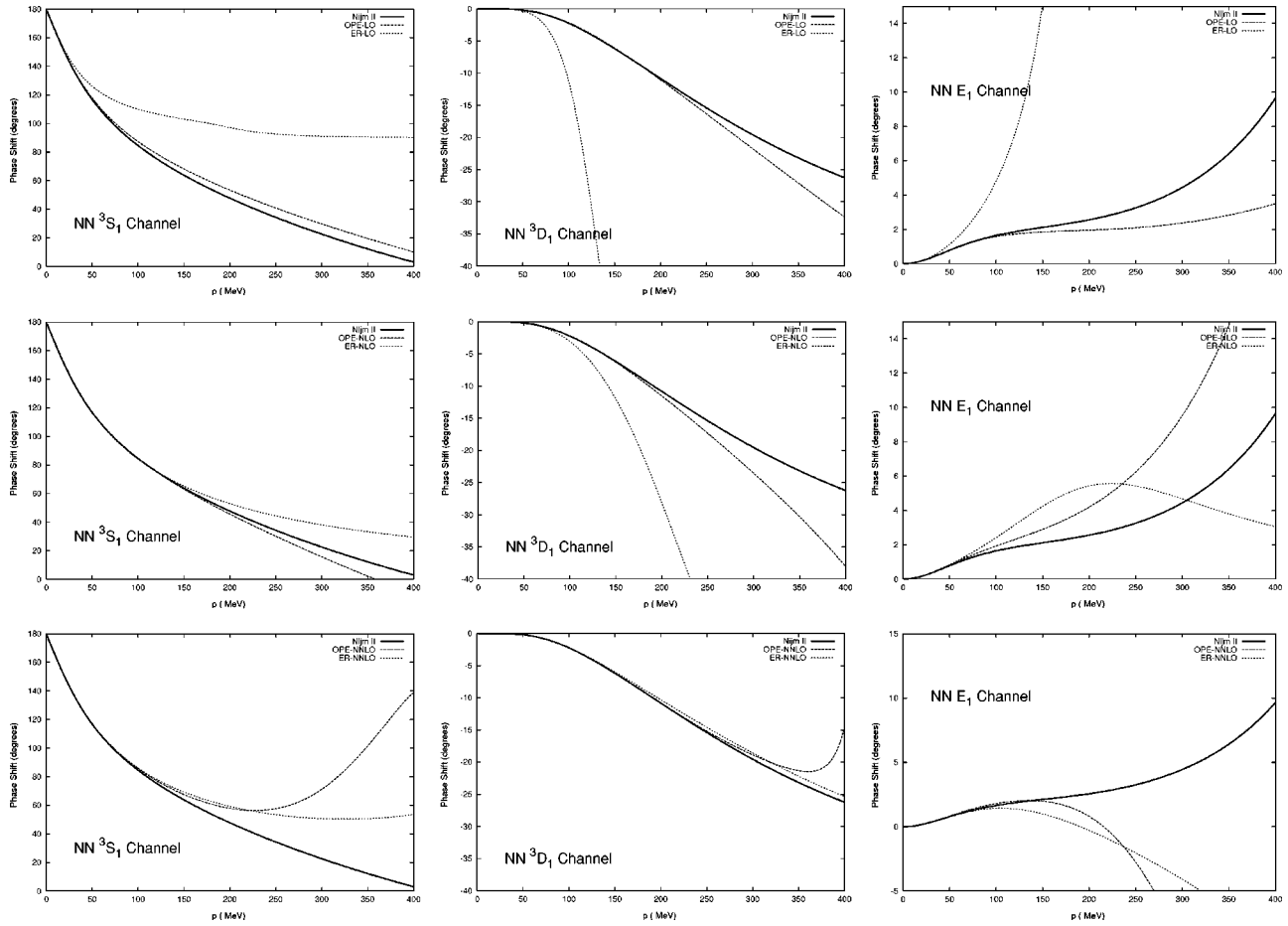

FIG. 5. The effect of including the OPE potential on top of the effective range expansion (ERE). Top panel: $^3S_1$, $^3D_1$, and E_1 at LO with (OPE-LO) and without (ER-LO) OPE explicit effects. Middle panel: same but for NLO. Bottom panel: same but NNLO. The difference between ER and OPE indicates the size of the explicit effects due to the OPE potential to LO (contact terms), NLO (k^2 terms), and NNLO (k^4 terms). In both cases the low energy threshold parameters coincide with those extracted from the NijmII potential. Data are the PWA from Refs. [33,34].

variations in R_S may generate large changes in the phase shifts at $k \sim m_\pi$. This is mainly due to the onset of limit cycles at short distances.

D. Are pions perturbative?

The discussion of which power counting is the appropriate one for the *NN* interaction corresponds physically to the question whether or not the pion cloud can be considered to be perturbative. It is important to realize that within our framework we are considering OPE departures from the effective range expansion to a given order. Thus, at sufficiently low k explicit pion effects can always be considered perturbative. This is so regardless of the number of k^2 terms included in the initial condition. Actually, the point is rather if the low energy threshold parameters can be considered large or small. According to our results in Fig. 5 it seems that the best possible agreement can be obtained when both the scattering lengths and the effective ranges are taken to be large, while other low energy parameters can be taken to be small. This can be seen in Fig. 5 where the effects of including OPE are compared to the ERE to LO, NLO, and NNLO. Given this fact we expect a kind of consistent long distance perturbation theory to work. The details of such an expansion will be presented elsewhere.

E. Evolution of the short distance boundary condition

As we have said, the short distance singularity of the OPE potential enforces a very precise determination of the running low energy threshold parameters at short distances, and hence of the boundary condition. We can directly determine this dependence by using Eq. (55) and Eq. (58). For simplicity and to illustrate the point we just display in Fig. 6 the behavior of the boundary condition parameters as a function of the short distance boundary radius in the zero energy limit, both for the singlet $^1S_0$ and triplet $^3S_1$ channel without mixing and for the triplet $^3S_1$-$^3D_1$ channel. The fixed point and limit cycle behavior obtained for the running of the low energy threshold parameters maps into a similar behavior for the short distance boundary condition. From the picture it is clear that the standard procedure of integrating the Schrödinger equation upwards from a given short distance boundary radius to infinity in order to fit the low energy

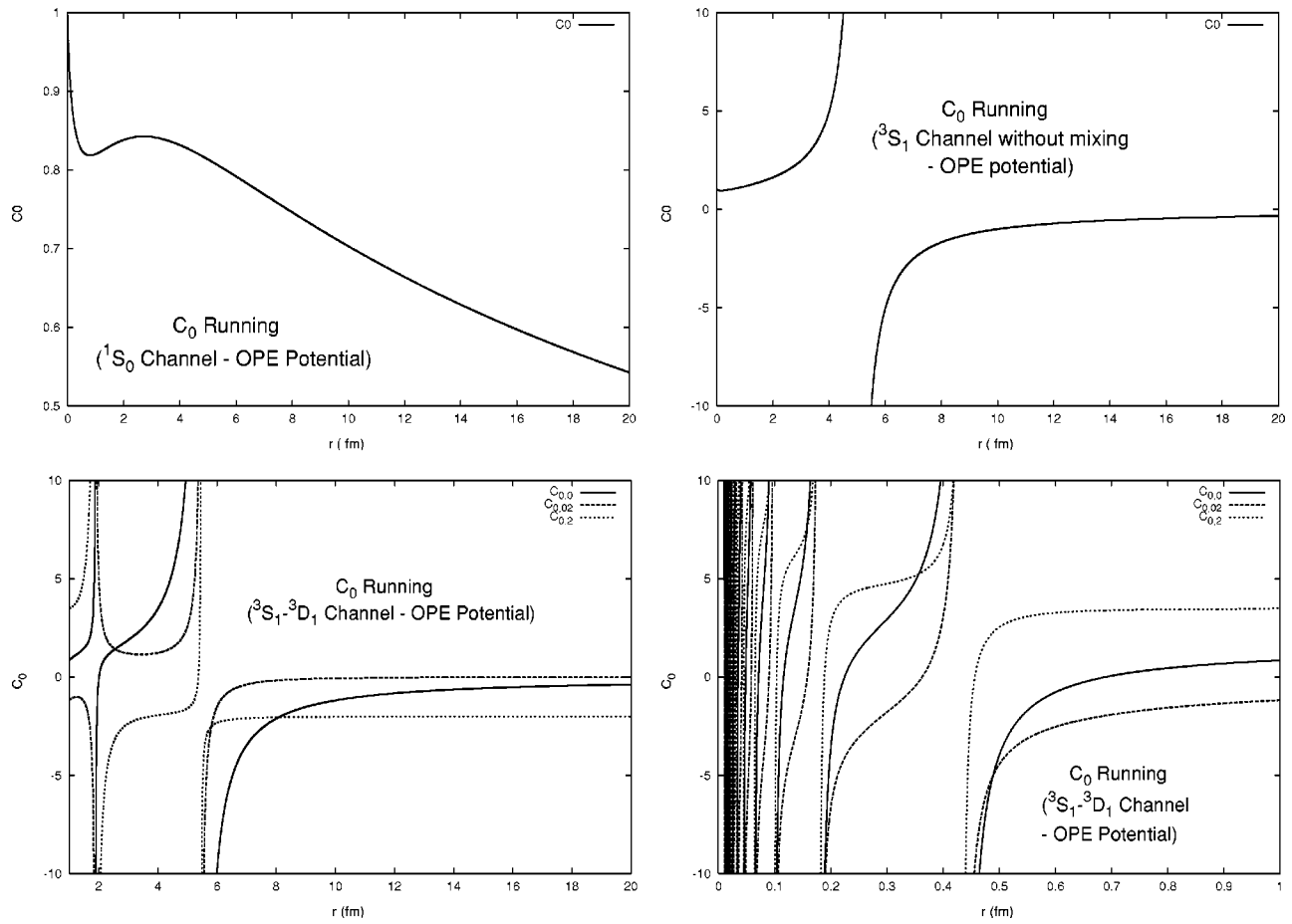

FIG. 6. Evolution of the dimensionless short distance boundary conditions at zero energy $\mathbf{C}_0(R)=\mathbf{1}-R\mathbf{L}_0(R)=\mathbf{1}-R\mathbf{u}_0'(R)\mathbf{u}_0(R)^{-1}$ with the boundary radius R due to OPE potential. Top: Singlet ${}^1S_0$ channel (left) and triplet ${}^3S_1$ channel (right) without mixing using Eq. (55). Bottom: The triplet ${}^3S_1$-${}^3D_1$ channel. The coefficients C^0_{ss}, C^0_{sd}, and C^0_{dd} are related to the running scattering lengths α_{00}, α_{02}, and α_{22} through Eq. (58). Large scale (left) and enlarged (right) picture.

parameters would require a very high precision determination of a rapidly varying boundary condition in the case of the triplet ${}^3S_1$-${}^3D_1$ channel. It is clear that a determination of the C_0 constants from a fit to the phase shifts in the low energy region would be extremely delicate in the limit $R_c \to 0$ in practice. Instead, the present approach computes directly the boundary condition in a power expansion of the energy at any given radius from the physical values of the low energy parameters. Actually, our method is equivalent to integrate the Schrödinger equation from that short distance boundary radius to infinity. In addition, the singular and attractive nature of the OPE potential allows a WKB treatment of the short distance singularity, and allows elimination of the finite cutoff radius taking the limit $R_c \to 0$. Obviously, the present framework can be extended to reanalyze the role of TPE potentials in a nonperturbative way and completely free of finite cutoff artifacts, where the short distance behavior is qualitatively similar.[7]

[7]Unlike the OPE where one has both an attractive and repulsive $1/r^3$ singularity (see Sec. IV), in the TPE case one encounters attractive $1/r^6$ singularities for coupled channels.

VI. CONCLUSIONS

In the present paper we have analyzed the renormalization of the OPE interaction in the presence of contact and derivative interactions of any order for *NN* scattering both for the singlet and triplet channel states. The basic point of our approach is to regularize the *unknown* short distance physics by means of a boundary condition at a certain boundary radius, above which the OPE potential is assumed to work, i.e., where pions are treated explicitly. Below that scale pions contribute implicitly to the scattering properties although always in combination with other effects that cannot be disentangled unless a given distance scale is specified. Actually, when the boundary radius goes to infinity, above the pion Compton wavelength, we have a low energy theory of contact interactions and derivatives thereof. As the boundary radius goes below the OPE range, we have a theory where pions are eliminated above the scale set by the boundary. This allows us to remove explicitly pion effects in the threshold parameters for the OPE potential in an unambiguous and model independent way. The renormalization group flow implied by our nonperturbative equations is unique provided the OPE potential is assumed to be valid all the way down to

the origin. This is obviously not a realistic assumption but it is absolutely necessary to go to these small distances in order to get rid of any finite short distance cutoff effect and properly define the OPE contributions to the scattering observables. This result fully complies with the spirit of an effective field theory: the terms in a low momentum expansion of the amplitude are shape independent, while the remaining powers depend both on the long distance OPE details (like the left branch cut) and the shape independent low energy parameters themselves.

The short distance behavior of threshold parameters present either an ultraviolet fixed point structure in the $^1S_0$ and $^3S_1$-without-mixing channels, whereas we find limit cycles for the $^3S_1$-$^3D_1$ channel due to the singular and attractive behavior of the OPE contribution to the tensor potential. This means that in the latter case there is not a monotonic trend at short distances. A direct consequence of having both ultraviolet fixed points and limit cycles for the threshold parameters is that a delicate fine tuning of the short distance physics is implied. In addition, for the experimental values of the threshold parameters one obtains huge changes for distances below 2 fm when OPE effects are removed. Nevertheless, we find moderate changes in the phase shifts due to explicit pion effects. Actually, in the $^1S_0$ and $^3S_1$-without-mixing channels the effect is found to be compatible with a perturbative treatment. In the $^3S_1$-$^3D_1$ channel the effect is a bit more complicated due to the presence of ultraviolet limit cycles triggered by the singular character of the tensor potential; the coupled channel amplitudes are nonperturbatively renormalizable while they become perturbatively nonrenormalizable. This makes a naive perturbative treatment slightly more subtle. One of the advantages of having a renormalizable theory is that nonperturbative equations make sense, and any perturbative treatment should arise as a controllable approximation to the full equations. As we have pointed out along the paper, this is probably an advantage of using coordinate space methods and a boundary condition renormalization versus momentum space methods.

Taking into account all the nice features of the present calculation, in particular, getting a handle on the finite cutoff corrections, the results presented in this paper are very satisfactory, suggesting several improvements. Explicit two-pion exchange contributions are expected to contribute significantly at about 1.5–2 fm at the level of the potential, so our results for the evolution of the threshold parameters should not be considered realistic below that scale, or equivalently above c.m. momenta of about 100–150 MeV, as it seems to be the case. In addition, our description should be enlarged to include higher partial waves. For peripheral waves one expects perturbative methods to work since there is a strong centrifugal suppression of the wave function at the origin, and perturbative renormalization methods can be applied. For those the present approach does not have much to say. Low partial waves, however, are particularly interesting since a resummation of pion exchanges seems crucial to understand the data. Work along these lines will be presented elsewhere [43].

Note added. Recently the work of Ref. [40] appeared on the web. There, their previous work was extended to take into account also attractive $1/r^2$ potentials. The mixed boundary condition plays an essential role.

ACKNOWLEDGMENTS

We thank J. Nieves for discussions. This work is supported in part by funds provided by the Spanish DGI Grant No. BMF2002-03218, Junta de Andalucía Grant No. FM-225, and EURIDICE Grant Number HPRN-CT-2003-00311.

APPENDIX: DETERMINATION OF LOW ENERGY PARAMETERS AND THE THEORY WITHOUT EXPLICIT PIONS

An essential ingredient of our formalism is to parameterize the scattering data directly in terms of low energy threshold parameters, such as α, r, and v, defined through Eq. (29). Unfortunately, besides α and r_0 in the singlet and triplet channels, the PWA database [33,34] does not provide values for them. In principle they could be obtained directly from a fit to the *NN* data base in the pertinent channels, at sufficiently low energies. Such a procedure turns out to be numerically unstable, particularly for the v parameter, because it depends very strongly on the energy window chosen for the fit. We have also tried, with no success, other methods for the determination of the low energy threshold parameters, such as evaluation of derivatives within several algorithms. The reason for the failure has to do with round-off errors generated by the relatively small number of digits provided in the *NN* database. On the other hand, the *NN* database provides explicit potentials, some of them local such as the NijmII and Reid93 potentials, for which the variable phase approach may directly be applied. In such a way we can uniquely and accurately determine all the needed low energy threshold parameters by integrating Eqs. (40) *upwards* from the origin to infinity with trivial boundary conditions. Our results can be summarized as follows for the NijmII and the Reid93 (in brackets) potential.

(1) Singlet $^1S_0$ NijmII (Reid93):

$$\alpha_0 = -23.74(3),\ r_0 = 2.67(75),\ v_2 = -0.48(9). \quad \text{(A1)}$$

(2) Triplet $^3S_1$ without mixing NijmII (Reid93):

$$\alpha_0 = 5.001(3),\ r_0 = 1.833,\ v_2 = 0.131(41). \quad \text{(A2)}$$

(3) Triplet $^3S_1$-$^3D_1$ with mixing NijmII (Reid93):

$$\mathbf{a} = \begin{pmatrix} 5.419(22) & 1.647(6) \\ - & 6.504(453) \end{pmatrix}, \quad \text{(A3)}$$

$$\mathbf{r} = \begin{pmatrix} 1.833 & 0.404(12) \\ - & -3.522(66) \end{pmatrix}, \quad \text{(A4)}$$

$$\mathbf{v} = \begin{pmatrix} -0.131(41) & -0.274(64) \\ - & -3.70(80) \end{pmatrix}. \quad \text{(A5)}$$

The $^3S_1$ channel without mixing parameters has been obtained from the $^3S_1$-$^3D_1$ channel for the $^3S_1$ component and $\alpha_0 = 1/(\mathbf{a}^{-1})_{00}$, complying with the low energy expansion of the **M** matrix, Eq. (29) (although we will be using the NijmII parameters).

Once the threshold parameters have been determined, we can use the coupled channel effective range expansion, Eq. (29), to find out to what extent this expansion applies. On theoretical grounds we expect this expansion to converge within the region of analyticity of the S matrix, which presents a left cut at $k=\pm i m_\pi/2$. In Fig. 5 we compare the quality of the ERE including LO, NLO, and NNLO contributions to the original data of Refs. [33,34]. As we see, to describe the data within the ERE approach up to the convergence radius $m_\pi/2$ one has to go at least to NLO. The description of the data below $m_\pi/2$ is improved, as expected, with higher orders in the ERE. Above this region, where OPE should play a role, this is not necessarily so. Actually, we see that in the $^3S_1$ and E_1 channels the NNLO is worse than the NLO approximation.

[1] S. Weinberg, Phys. Lett. B **251**, 288 (1990); Nucl. Phys. **B363**, 3 (1991).
[2] C. Ordonez, L. Ray, and U. van Kolck, Phys. Rev. C **53**, 2086 (1996); Phys. Rev. Lett. **72**, 1982 (1994); C. Ordonez and U. van Kolck, Phys. Lett. B **291**, 459 (1992).
[3] T. S. Park, K. Kubodera, D. P. Min, and M. Rho, Phys. Rev. C **58**, 637 (1998).
[4] E. Epelbaum, W. Glockle, and U. G. Meissner, Nucl. Phys. **A637**, 107 (1998); E. Epelbaum, W. Glockle, A. Kruger, and U. G. Meissner, *ibid.* **A645**, 413 (1999); E. Epelbaum, W. Glockle, and U. G. Meissner, *ibid.* **A671**, 295 (2000).
[5] D. B. Kaplan, M. J. Savage, and M. B. Wise, Nucl. Phys. **B534**, 329 (1998); Phys. Lett. B **424**, 390 (1998); Nucl. Phys. **B478**, 629 (1996).
[6] J. Gegelia, Contributed to Workshop on Methods of Nonperturbative Quantum Field Theory, Adelaide, Australia, February 1998, in *Adelaide 1998, Nonperturbative Methods in Quantum Field Theory*, pp. 30–35, Phys. Lett. B **429**, 227 (1998); **463**, 133 (1999).
[7] S. Fleming, T. Mehen, and I. W. Stewart, Nucl. Phys. **A677**, 313 (2000); Phys. Rev. C **61**, 044005 (2000).
[8] M. C. Birse, J. A. McGovern, and K. G. Richardson, Phys. Lett. B **464**, 169 (1999).
[9] T. Barford and M. C. Birse, in *A renormalization-group approach to two-body scattering with long-range forces*, AIP Conf. Proc. No. 603 (AIP, New York, 2001), p. 229.
[10] T. Barford and M. C. Birse, Phys. Rev. C **67**, 064006 (2003).
[11] H. van Haeringen and L. P. Kok, Phys. Rev. A **26**, 1218 (1982).
[12] D. B. Kaplan, M. J. Savage, and M. B. Wise, Nucl. Phys. **B478**, 629 (1996).
[13] S. R. Beane, P. F. Bedaque, M. J. Savage, and U. van Kolck, Nucl. Phys. **A700**, 377 (2002).
[14] P. F. Bedaque and U. van Kolck, Annu. Rev. Nucl. Part. Sci. **52**, 339 (2002).
[15] J. F. Yang, nucl-th/0310048.
[16] J. Gegelia and S. Scherer, nucl-th/0403052.
[17] D. R. Phillips, S. R. Beane, and T. D. Cohen, Nucl. Phys. **A631**, 447C (1998).
[18] T. Mehen and I. W. Stewart, Phys. Rev. C **59**, 2365 (1999).
[19] T. Mehen and I. W. Stewart, Phys. Lett. B **445**, 378 (1999).
[20] T. D. Cohen, B. A. Gelman, and U. van Kolck, Phys. Lett. B **588**, 57 (2004).
[21] T. Frederico, V. S. Timoteo, and L. Tomio, Nucl. Phys. **A653**, 209 (1999).
[22] J. Gegelia and G. Japaridze, Phys. Lett. B **517**, 476 (2001).
[23] D. Eiras and J. Soto, Eur. Phys. J. A **17**, 89 (2003).
[24] J. A. Oller, Nucl. Phys. **A725**, 85 (2003).
[25] D. B. Kaplan, Nucl. Phys. **B494**, 471 (1997).
[26] J. Nieves, Phys. Lett. B **568**, 109 (2003).
[27] E. Epelbaum, W. Gloeckle, and U. G. Meissner, Eur. Phys. J. A **19**, 401 (2004).
[28] E. Lomon and H. Fesbach, Rev. Mod. Phys. **39**, 611 (1967).
[29] D. R. Phillips and T. D. Cohen, Phys. Lett. B **390**, 7 (1997).
[30] T. D. Cohen and J. M. Hansen, Phys. Lett. B **440**, 233 (1998).
[31] U. van Kolck, Nucl. Phys. **A645**, 273 (1999).
[32] H. A. Bethe, Phys. Rev. **76**, 38 (1949).
[33] V. G. Stoks, R. A. Kompl, M. C. Rentmeester, and J. J. de Swart, Phys. Rev. C **48**, 792 (1993).
[34] V. G. J. Stoks, R. A. M. Klomp, C. P. F. Terheggen, and J. J. de Swart, Phys. Rev. C **49**, 2950 (1994); http://www.nn-online.org.
[35] M. C. M. Rentmeester, R. G. E. Timmermans, J. L. Friar, and J. J. de Swart, Phys. Rev. Lett. **82**, 4992 (1999).
[36] M. Pavon Valderrama and E. Ruiz Arriola, Phys. Lett. B **580**, 149 (2004).
[37] F. Calogero, *Variable Phase Space Approach to Potential Scattering* (Academic, New York, 1967).
[38] J. V. Steele and R. J. Furnstahl, Nucl. Phys. **A645**, 439 (1999).
[39] S. R. Beane, P. F. Bedaque, L. Childress, A. Kryjevski, J. McGuire, and U. v. Kolck, Phys. Rev. A **64**, 042103 (2001).
[40] T. Barford and M. C. Birse, nucl-th/0406008.
[41] E. Braaten and H. W. Hammer, Phys. Rev. Lett. **91**, 102002 (2003).
[42] S. Albeverio, F. Gesztesy, R. Hoegh-Krohn, and H. Holden, *Solvable Models in Quantum Mechanics*, Texts and Monographs in Physics (Springer, New York, 1988).
[43] M. Pavón Valderrama and E. Ruiz Arriola (in preparation).
[44] G. L. Shaw and M. L. Ross, Ann. Phys. (N.Y.) **13**, 147 (1961).
[45] A. M. Badalian, L. P. Kok, M. I. Polikarpov, and Y. A. Simonov, Phys. Rep. **82**, 31 (1982).
[46] T. D. Cohen and J. M. Hansen, Phys. Rev. C **59**, 13 (1999).
[47] T. D. Cohen and J. M. Hansen, Phys. Rev. C **59**, 3047 (1999).
[48] D. R. Entem and R. Machleidt, Phys. Lett. B **524**, 93 (2002).